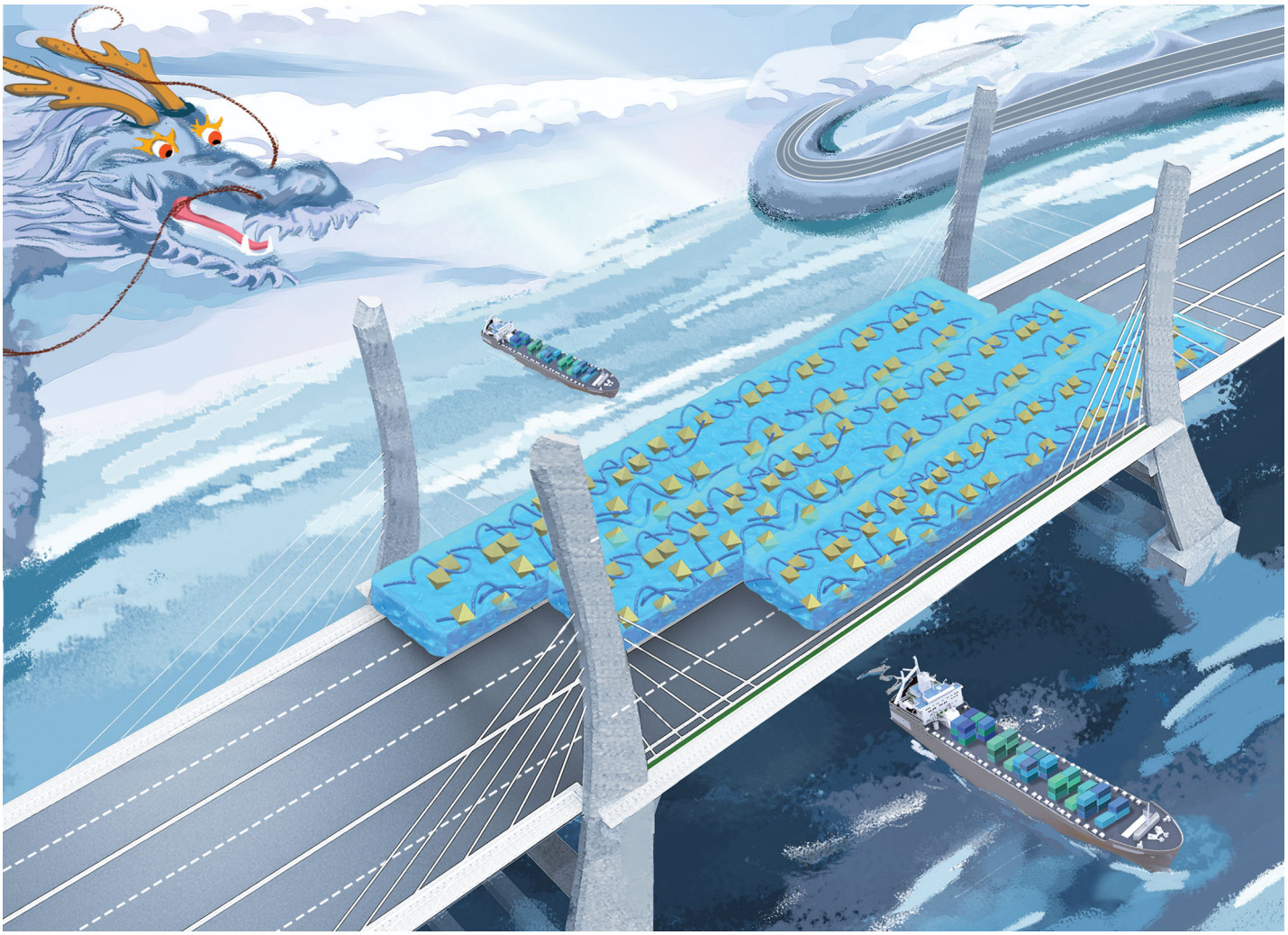

Showcasing research from the laboratory of Professor Wei Zhang, Professor Jiaping Liu and Professor ZhengMing Sun, School of Materials Science and Engineering, Southeast University, Nanjing, China.

Hydrogel networks as underwater contact adhesives for different surfaces

Underwater adhesives with intrinsically tough and stable performance are urgently needed for environmental and engineering applications. This work develops a universal strategy wherein hydrogels are tuned into underwater adhesives by dynamic interactions with nanocrystals, having profound implications to broaden the emerging applications of hydrogel materials.

As featured in:

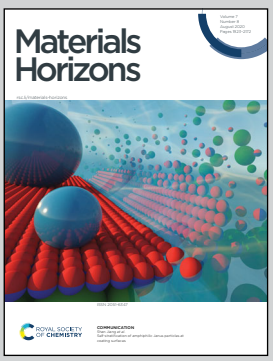

See Jiaping Liu, ZhengMing Sun, Wei Zhang *et al.*, *Mater. Horiz.*, 2020, **7**, 2063.

ROYAL SOCIETY OF CHEMISTRY

rsc.li/materials-horizons

Registered charity number: 207890

Materials Horizons

ROYAL SOCIETY OF CHEMISTRY

COMMUNICATION

View Article Online
View Journal | View Issue

Cite this: *Mater. Horiz.*, 2020, 7, 2063

Received 3rd February 2020, Accepted 19th June 2020

DOI: 10.1039/d0mh00176g

rsc.li/materials-horizons

Hydrogel networks as underwater contact adhesives for different surfaces†

Feng Pan,‡[abc] Shaoxiong Ye,‡[a] Ruixing Wang,[a] Wei She,[ac] Jiaping Liu,*[ac] ZhengMing Sun*[b] and Wei Zhang*[b]

Underwater adhesives with intrinsically tough and stable performance are urgently needed for environmental and engineering applications. Marine organisms have inspired numerous studies on the design and development of wet adhesives. Here we report a facile yet powerful strategy that recapitulates the delivery process of mussel adhesion for the development of strong and durable hydrogel adhesives. With the hydrogel matrix serving as an interfacial binding site, while the nanocrystal fillers contribute to the strong cohesion, they demonstrate outstanding adhesion abilities to a wide range of wet surfaces including aluminum, ceramics, glass, polymers and wood. Moreover, in contrast to commercial products for underwater bonding, the hydrogel adhesives present continuous strength growth instead of degradation with time due to the hydration effects and intrinsic reinforcement capabilities of ye'elimite. By synergistically combining macroscopic scale architectures and molecular level interactions, this *in situ* formation strategy opens a new route to incorporate nanocrystals into a hydrogel matrix, leading to a universal bonding solution on diverse surfaces underwater.

New concepts

The adhesive plaques of mussels have inspired many synthetic underwater adhesives, which usually contain catechol functional groups. However, they require sophisticated chemical synthesis and suffer from oxidation-induced adhesion diminishment. By recapitulating the delivery process of mussel adhesion, we developed a facile yet powerful solution for bonding diverse materials underwater with a nanocrystal crosslinked hydrogel that renders robust interaction and fast regulation. Unlike most synthetic adhesives that treat water or moisture as a surface contaminant, this hydrogel utilizes water to generate nanocrystals that reinforce the polymer matrix and enhance the interfacial reaction. Therefore, instead of losing bonding capability with time like ordinary glues, our system gains sustainable strength growth upon use under wet conditions. This work develops a universal strategy wherein hydrogels are tuned into underwater adhesives by dynamic interactions with nanocrystals, having profound implications to broaden the emerging applications of hydrogel materials.

Strong, fast and stable underwater adhesion has been a major challenge in adhesion science and engineering,[1–3] as water creates a weak boundary layer that may prevent direct surface contact between the adhesives and substrates, leading to the diminishment of surface energy and deterioration of the adhesion strength. As a result, how to effectively repel water molecules between the two surfaces is the key to establish robust bonding under wet conditions. Marine organisms, such as mussels, sandcastle worms and barnacles, are naturally equipped with reliable strategies to achieve interfacial adhesion under dynamic and turbulent environments.[4–6] 3,4-Dihydroxy-L-phenylalanine (DOPA), a catecholic amino acid, presented in their adhesive proteins, has been identified to be able to penetrate water boundary layers, and subsequently interact with the local metal ions Fe^{3+}, Mg^{2+} and Zn^{2+} to form adhesive bonds with the substrates.[7] Since then, catechol moieties have been exploited as a popular route for the design and development of biomimic wet adhesives.[5] Most of the catechol-based adhesives require either sophisticated chemical synthesis or delicate reaction conditions,[8–12] which significantly limits their potential for practical applications. Moreover, they often suffer from performance degradation upon oxidation. Therefore, we decided to investigate whether a synthetic system that is completely irrelevant to catechol moieties could also unlock the mussel's functional dynamics of effective underwater adhesion.

Here we have reported a facile yet powerful alternative to fabricate a bio-inspired underwater adhesive that renders robust interaction and fast regulation. Instead of mimicking the chemical structure of catechol molecules, our strategy

[a] *Jiangsu Key Laboratory of Construction Materials, School of Materials Science and Engineering, Southeast University, Nanjing, Jiangsu 211189, China. E-mail: ljp@seu.edu.cn, zmsun@seu.edu.cn, w69zhang@seu.edu.cn*

[b] *Jiangsu Key Laboratory of Advanced Metallic Materials, School of Materials Science and Engineering, Southeast University, Nanjing, Jiangsu 211189, China*

[c] *State Key Laboratory of High Performance Civil Engineering Materials, Nanjing, Jiangsu 210008, China*

† Electronic supplementary information (ESI) available. See DOI: 10.1039/d0mh00176g

‡ These authors contributed equally to this work.

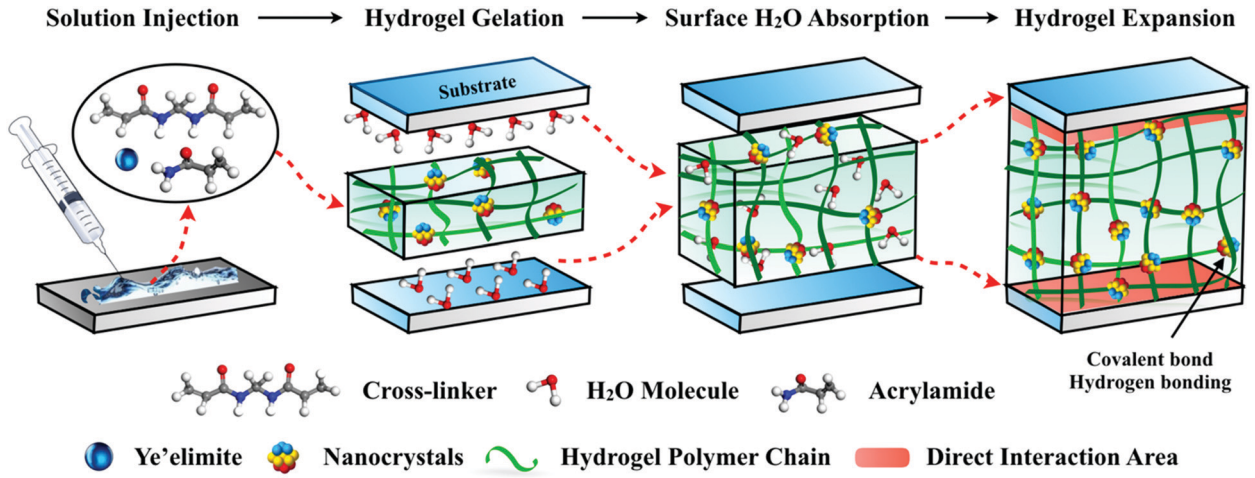

Fig. 1 Design of nanocrystal reinforced hydrogel networks. The monomer, crosslinker, and ye'elimite were simply blended to fabricate a nanocomposite PAM hydrogel solution, which was directly injected under water to the substrates. During gelation, the water molecules at the interfaces were captured into the hydrogel matrix, forming a sound bonding between the adhesives and the substrates.

leverages on the elegant cooperation of macroscopic scale architectures (organic–inorganic complex and multi-scale design) and molecular level interactions (crosslinking through ionic and hydrogen bonding). It recapitulates the whole delivery process of mussel adhesion: mussels secret adhesive proteins at the surface/interface (to establish the adhesion), followed by hardening the adhesive plaques (to have a good cohesion) to perform robust bonding to the substrate.

The design mechanism of this underwater adhesive is illustrated in Fig. 1. We started with the simple blending of the monomer (acrylic amide), crosslinker (*N*,*N*′-methylene acrylamide), and inorganic filler ye'elimite ($Ca_4(AlO_2)_6SO_3$) to form a nanocomposite poly(acrylic amide) (PAM) hydrogel precursor, which can be injected directly onto the substrate surfaces under wet conditions. The hydrophilic hydrogel matrix can absorb and squeeze out the surface water by swelling, and subsequently penetrate the water boundary layer. The key aspect in this strategy is to adopt the fast hydration process of ye'elimite to generate ettringite and $Al(OH)_3$ nanocrystals for polymer crosslinking, and to take advantage of the hydration process to accelerate the solidification of the hydrogel.

The feasibility of this key aspect is verified by isothermal calorimetry measurement, by which the heat released was monitored as a function of time during the hydration (or gelation) of adhesives, the ye'elimite paste and the pure hydrogel (Fig. S1, ESI†). The pure hydrogel exhibits a single peak at around 2.3 h, which corresponds to its gelation time. Two characteristic peaks are observed during the hydration of the nanocomposite adhesive, the first of which coincides with the dissolution peak of ye'elimite at the very beginning, and the main peak corresponds to a massive polymerization process (Fig. S1(a), ESI†) with a significantly higher value compared to the pure hydrogel. In addition, the cumulative heat released from ye'elimite hydration accounts for around 16% of the total heat released from the adhesive within the same time frame (Fig. S1(b), ESI†). All these phenomena suggest that the gelation of the hydrogel is very likely to be accelerated by the heat released from ye'elimite hydration. Another plausible explanation could be related to the presence of trace transition metals Fe and Ti detected by X-ray florescence (XRF) and X-ray microanalysis *via* SEM (Fig. S2, ESI†). The presence of Fe and Ti may cause a rapid decomposition of APS, which produces more radicals to accelerate the polymerization process of the hydrogel.

Upon forming ionic or metal-chelating bonds with the inorganic nanocrystals, the adhesives are rapidly solidified within 8 minute, establishing a strong interfacial adhesion between the two adherent surfaces. The incorporation of nanocrystals with different sizes and shapes in the hydrogel matrix may give rise to a multi-scale design with the interplay of ionic interactions or hydrogen bonding, which contributes to the gelation process and they act as physical crosslinkers. With the hydrogel matrix serving as a binding site while the nanocrystal fillers contributing to the strong cohesion, the hybrid adhesives possess elevated mechanical properties and are able to maximize the energy consumption during debonding. Utilizing inorganic nanoparticles to strengthen the mechanical properties of the hydrogel has also been reported by Haraguchi *et al.*[13] and Rose *et al.*[14]

At the interface between the adhesives and the substrates, water molecules are absorbed and trapped by the hydrogel in a rapid manner to enlarge the effective contact area. Unlike most synthetic adhesives where water or moisture acts as a surface contaminant to reduce the contact adhesion,[15,16] the hydrogel-based composite adhesives require the existence of water. Water is a prerequisite component for the hydration of ye'elimite, through which the adhesion strength of the matrix is developed, and the strong impingement at the interface is achieved due to the formation of nanocrystals. Therefore, the long-lasting immersion in water guarantees the sustainable strength growth of the matrix, instead of diminishing the adhesion performance as it does to conventional underwater adhesives.[17]

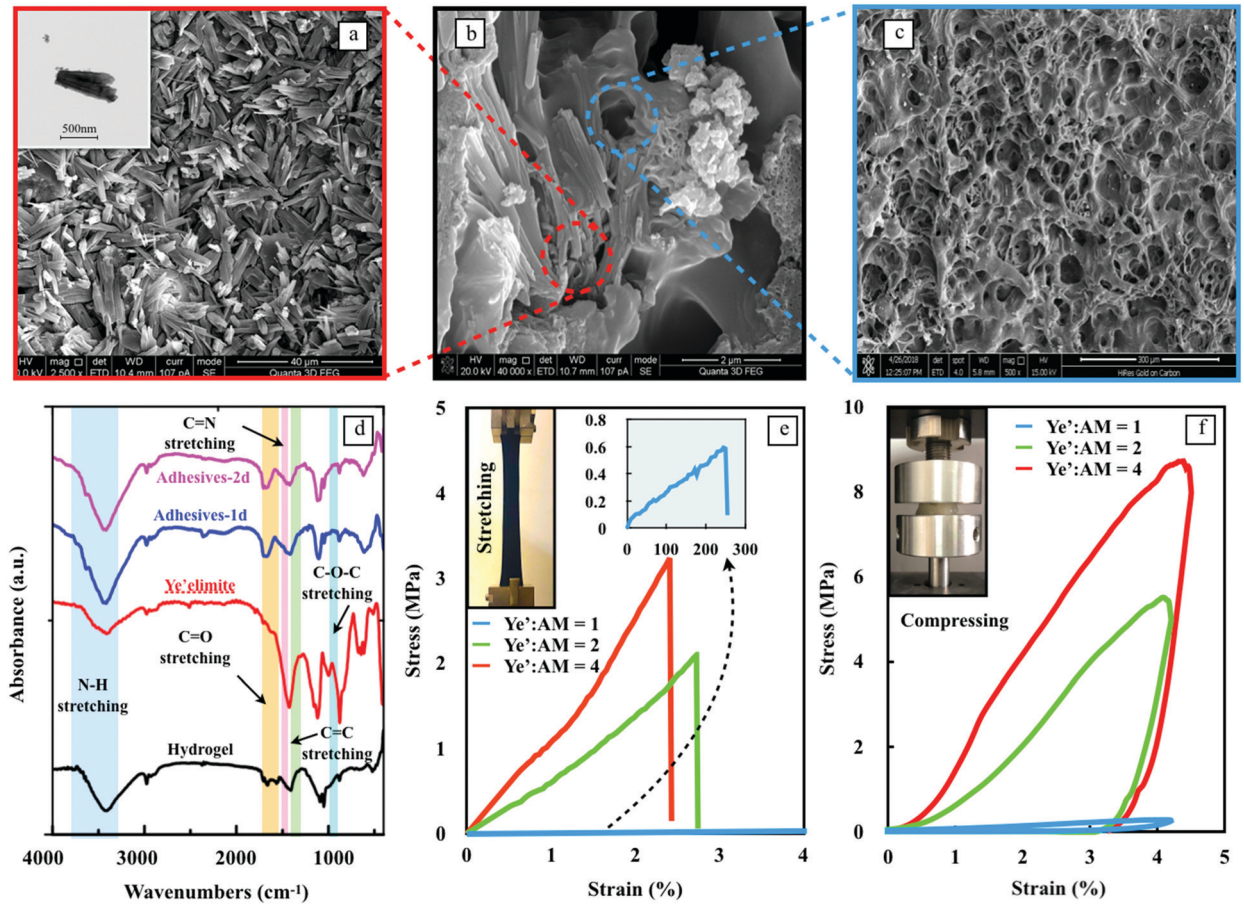

Fig. 2 Characterization details of nanocomposite adhesives. (a) SEM image of the hydrated ye'elimite paste. The inset image on the upper left is the TEM image of nano crystals contained in nanocomposite adhesives. (b) SEM image of nanocomposite adhesives and (c) solidified hydrogel. (d) Stress–strain curves of nanocomposite adhesives with different mass ratios of ye'elimite and AM under tension. Adhesives-1d and adhesive-2d in this image represent the adhesive samples cured for 1 day and 2 days, respectively. (e) Testing the tensile strength and irreversible deformation of the hydrogel. (f) Stress–strain curves of nanocomposite adhesives with different mass ratios of ye'elimte and AM under cyclic compressions.

The design of biomimetic hydrogels with exceptional adhesive properties was based on two key principles, one of which was the construction of a unique 3D architecture. Fig. 2a shows the microstructure of the hydrated ye'elimite paste, which has a homogenous and dense distribution of needle-shape nanocrystals in the size range of 10 to 30 μm (inset TEM image). Upon incorporation into the hydrogel matrix, the nanocomposite features interconnected networks composed of thin PAM walls with nanocrystals grown inside (Fig. 2b), leading to a mechanically reinforced system. The SEM image in Fig. 2c indicates that the pure PAM hydrogel possesses a crosslinked network with multi-porous structures, demonstrating that the hydration of ye'elimite does not influence the gelation behavior of the PAM polymer chains.

Another key point of the hydrogel design was the *in situ* formation of ettringite and $Al(OH)_3$ nanocrystals, which was applied to crosslink the hydrogel network in the presence of water. In summary, two major chemical reactions are involved during the solidification of nanocomposite adhesives: (a) AM and MBA underwent free radical polymerization, in which AM monomers formed linear chains and MBA aided to form cross-linked polymer matrices; (b) hydration of ye'elimite as described in eqn (1). These two reactions take place simultaneously since mixing. In addition, the nano crystals generated gradually during the hydration of ye'elimite would reinforce the matrix of the hydrogel, yielding a rigid skeleton with extraordinary mechanical properties. It should be mentioned that at the very beginning, due to the low hydration degree of ye'elimite, there were not many nanoparticles available. It is the gelation of the hydrogel, in the presence of MBA, that binds the mixing paste together under water. Then with the continuous hydration of Ye'elimite, more nanoparticles are generated and gradually form a stiff skeleton, strengthening the mechanical properties of the adhesive.

$$Ca_4(AlO_2)_6SO_4 + 2CaSO_4{\cdot}2H_2O + 22H_2O \rightarrow Ca_6Al_2(SO_4)_3(OH)_{12}{\cdot}26H_2O + 2Al(OH)_3 \quad (1)$$

The interactions between the nanocrystals and the hydrogel were analyzed by FTIR (Fig. 2d) and XPS (Fig. S3, ESI†). The IR spectra of the nanocomposite exhibited characteristic peaks from each component; the band at 3418.70 cm^{-1} in the high-frequency region is characteristic of N–H stretching shifted

from 3410.53 cm^{-1} in the spectrum of the pristine hydrogel,[18] revealing the interaction between Al^{3+} and N–H groups. The peaks at 1705.09 cm^{-1} and 1049.58 cm^{-1} in the hydrogel spectrum are attributed to the C═O and C–O–C stretching vibrations,[19] which remained the same in the hybrid adhesives. The peaks at 1564.04 cm^{-1} and 1406.54 cm^{-1}, corresponding to C═N and C═C stretching vibrations from the hydrogel spectrum,[20] are integrated into a broad peak at 1420.18 cm^{-1} of the nanocomposite. This can be attributed to the crosslinking of the hydrogel polymer chains. The peaks at 1116.99 cm^{-1}, 881.34 cm^{-1} and 619.07 cm^{-1} are related to the asymmetric stretching vibration of S–O in the $[SO_4]$ group, the stretching vibration of Al–O in the $[AlO_4]$ group and the bending vibration of S–O in the $[SO_4]$ group from the ettringite.[21] In the XPS spectra (Fig. S3, ESI†), an intense N1s peak appeared at 397.5 eV. This is related to the formation of chemical bonding between the N–H bond of PAM and Al^{3+} bond of nanocrystals.[22] The latter is generated from ye'elimite hydration, as shown in the FTIR results above. With the strong covalent interactions, nanocrystals can act as effective crosslinkers to reinforce the host hydrogels.

The mechanical properties of the nanocomposite adhesives with three different ye'elimite-to-AM mass ratios were analyzed by tension and cyclic compression tests (Fig. 2e and f). Both tension and compression tests confirmed that the loading capacity of the hydrogel was improved significantly with the increase of ye'elimite content. Due to the intrinsic flexible characteristic of hydrogel materials, all the samples exhibit robust irreversibility under both tension and compression (inset images of Fig. 2e and f). Due to the superior performance of the nanocomposite adhesives, the curve of pure PAM is even lower than the curve of Ye' : AM = 1 and almost overlapped with the x-axis (tensile strength = 37.5 ± 2.0 kPa). Therefore, the pure PAM group is not plotted. It is worth mentioning that the ultimate strain of samples subjected to tension becomes 10 times less when the ye'elimite to AM ratio is larger than 2, which is related to the rigid skeleton formed by abundant nanocrystals within the hydrogel matrix. The substantial difference in the mechanical properties between the samples with Ye' : AM = 1 and 2 is indeed important evidence showing the beauty of the nanocomposite adhesives that utilize the nanocrystals generated from the hydration process of ye'elimite to form a stiff skeleton. With the increase of Ye' : AM from 1 to 2, the quantity of nanocrystals increases from a minor phase to a dominating phase in the microstructure, yielding a pronounced improvement in the mechanical properties.

As the design fully utilizes the merits of ye'elimite with its hydration effects and reinforcement capabilities, the nanocomposite hydrogel reveals remarkable wet adhesion properties. Fig. S4 (ESI†) qualitatively demonstrates the holding power of hydrogel-based adhesives in an aqueous environment. They were applied onto a small area under water and were able to hold various materials together. The remarkable underwater bonding performance of the nanocomposite adhesives can be attributed to a couple of prospects, one of them is related to the strong cohesion of the nanocomposite matrix, which is a function of time given that the hydration process of ye'elimite (eqn (1)) continuously yields nanocrystals in contact with water. Therefore, the matrix strength has a sustainable increase when the nanocomposite adhesives are used constantly under wet conditions. Ettringite and $Al(OH)_3$ nanocrystals gradually form a stiff skeleton that contributes to the strength of the system, while the soft hydrogel provides an energy dissipation mechanism during the debonding (Fig. 3a), which is essential to postpone the adhesion failure.

Another prospect is related to the adhesive interactions between the substrates and the adhesives at the interface. The nanocrystals generated from the hydration of ye'elimite can be easily precipitated on a wide range of surfaces, which enhances the effective contact interactions. Besides the improvement in the matrix strength, the nanocrystals can also contribute to anchoring the adhesives onto rough surfaces (Fig. 3b). The evidence of the anchorage effect was found *via* SEM (Fig. 3c) and 3D X-ray tomography (Fig. 3d). In addition, we used 180-grit and 800-grit papers to obtain aluminum substrates with two different roughness (R_a), 2.214 ± 0.643 μm and 1.174 ± 0.363 μm, measured by a nano 3D surface profilometer (CHOTEST SuperView W1, Fig. S5, ESI†). The adhesion strength was measured after 3 days of solidification. Nanocomposite adhesives applied on these two aluminum substrates exhibit an adhesion strength of 2.68 MPa and 3.31 MPa, respectively, showing 23.4% improvement on the rougher substrate, strengthening our proposed mechanism for physical anchoring.

Moreover, the hydrogel component absorbs water at the interface to maximize the contact area between the adhesives and the substrates. The adhesion performance P of the nanocomposite hydrogel, which could be either adhesion strength or bonding energy depending on specific cases, can be described by eqn (2):

$$P = \sum_{i=1}^{n} a_i C_i + \sum_{j=1}^{m} \beta_j A_j \quad (2)$$

where C_i and A_j represent the ith and jth contribution from the cohesion of the matrix (*i.e.*, the amount of the nanocrystals, the gelation of the hydrogel, the interaction between the nanocrystals and the hydrogel) and the adhesion at the interface (*i.e.*, chemical bonding between adhesives and substrates, anchorage, the physical interaction due to the presence of nanocrystals, and the effective contact area), respectively. The effective contact area depends on both the water absorption capacity of the hydrogel near the interface and also the surface roughness.[23,24] a_i and β_j quantify the corresponding contributions of C_i and A_j, and their values vary according to the substrates applied.

Eqn (2) provides an informative approach to assess the adhesion performance when the adhesives are applied upon different substrates. To quantify the adhesion strength of the nanocomposite hydrogel, we performed lap shear adhesion experiments on various substrates following the ASTM F2255-05 standard. The nanocomposite adhesive was applied onto the adherent substrates directly underwater using a plastic syringe (Movie S1, ESI†). The load of 1N was constantly applied on top

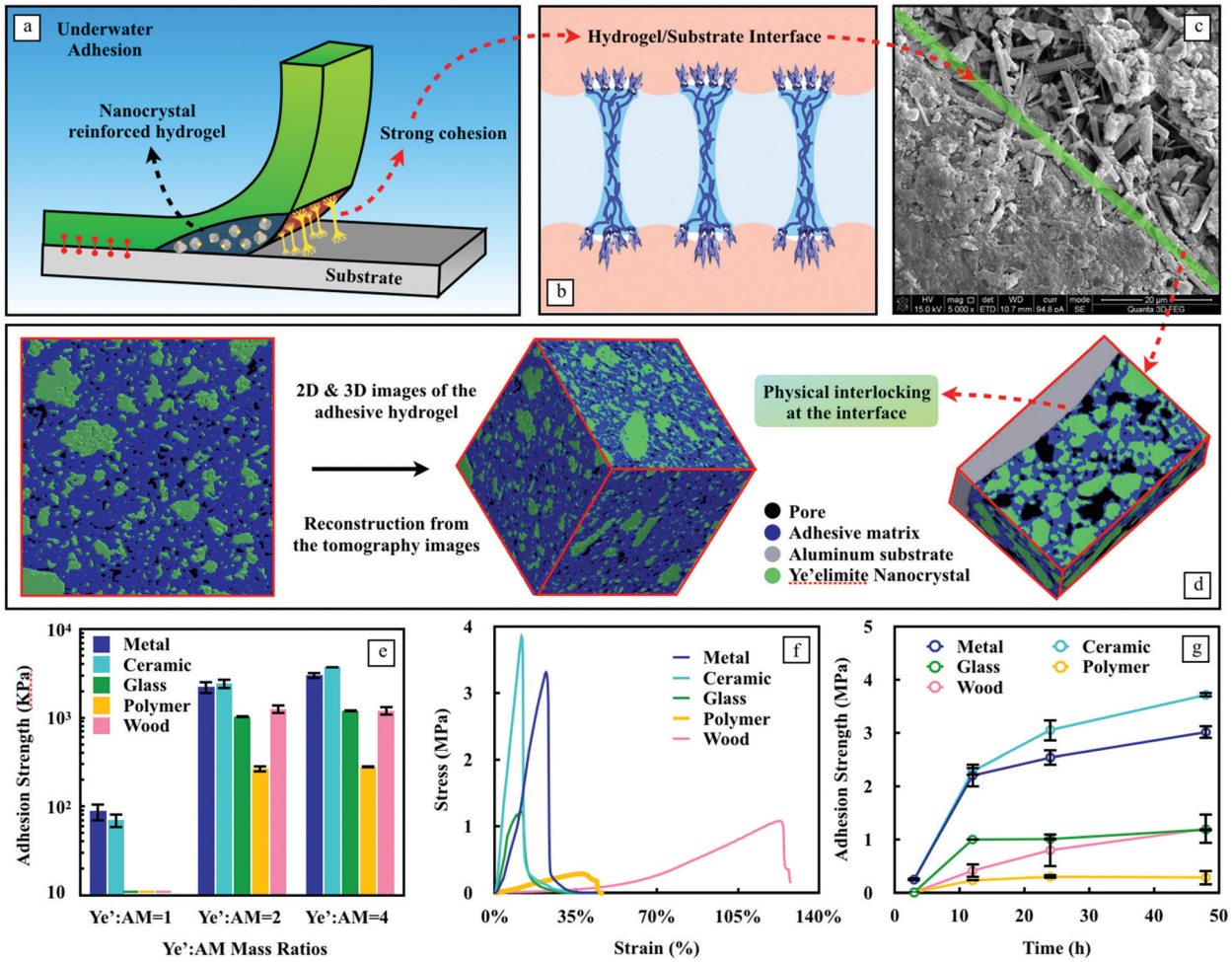

Fig. 3 Adhesion performance of nanocomposite adhesives and their failure behavior. (a) Schematic diagram showing the deformation evolution of nanocomposite adhesives during debonding from a substrate. (b) Schematic diagram showing the physical interlocking between the nanocrystals and the substrates, and (c) the corresponding SEM microscopy image at the interface. (d) 3D microstructure of nanocomposite adhesives measured *via* X-ray tomography, indicating the strong interaction between the adhesives and the Al substrate at the interface. (e) Influence of chemical compositions on the adhesion strength. Three mass ratios between ye'elimite and AM (1, 2, and 4) were adopted. (f) Stress–strain curves of nanocomposite adhesives applied on various substrates. (g) Development of underwater adhesion strength on multiple surfaces over time.

of the substrate to establish efficient contact, when the substrates bonded by the hydrogels were stored under water at 20 °C.

To better understand the contribution of each component to the cohesion and adhesion of the nanocomposite adhesives, three mass ratios between ye'elimite and AM were tested (Fig. 3e). When combined with AM, the gelation of AM to form a hydrogel inadvertently slows down the hydration of ye'elimite. This retarding effect is exaggerated with the increase of AM content. In agreement with Fig. 2d and e, ye'elimite not only improves the loading capacity of the nanocomposite adhesives (*i.e.*, the cohesion properties), but also boosts the adhesion strength (*i.e.*, the adhesion properties) universally on all the substrates tested in this study. This predominant effect of ye'elimite content on the adhesion strength can be attributed to its own hydration process which continuously yields a number of nanocrystals to both reinforce the matrix and to physically anchor onto the substrates.

Due to the superior mechanical and adhesion performances, and the higher potential on energy consumption during debonding considering the relatively higher hydrogel content, the mass ratio of ye'elimite to AM equal to 2 was adopted for the following tests. The stress–strain curves of adhesives on different substrates are shown in Fig. 3f, based on which the adhesion strength was assessed and listed in Table S1 (ESI†). Among all the substrates tested in this study, the nanocomposite adhesives exhibit strong adhesion on both ceramic and aluminum substrates, due to the preference of crystal precipitation and nucleation on these two substrates, resulting in the enhancement of chemical bonding between the adhesives and the substrates, thus improving the cohesion properties. Similar to ceramics and aluminum, glass is also considered as a type of hard material and can grow nanocrystals. However, due to the smooth characteristic of glass surfaces, the physical anchorage at the interface is weakened, which would impair the adhesion properties, in other words, reducing the values of A_i. Due to the

same reason, polytetrafluoroethylene (PTFE) with poor hydrophilicity showed the lowest adhesion strength among all the materials tested, with only 280.4 kPa after 24 h since application (Fig. 3g), which is still 60 times larger than gecko feet inspired underwater adhesives.[25] The hydrogels on wood exhibit the best deformation capability due to the mechanical anchorage from the adhesives to the rough surface and the large flexibility of the hydrogel in the matrix, the latter of which has been considered as the prevailing adhesion mechanism for wood bonding.[26] The adhesion strength of wood is about 3 times lower than that of ceramic and aluminum substrates. This is related to its inherent water sustaining capability due to the porous feature, which weakens the water adsorption of the hydrogel and reduces the effective contact area at the interface. However, the adhesion strength (1.194 MPa) on wood substrates underwater still exceeds that of the commonly used wood adhesives made of tannin and lignin-based materials measured under dry conditions (0.92 and 0.85 MPa, respectively).[27]

The nanocomposite adhesives experienced constant growth on all the tested substrates over time (Fig. 3g). Particularly for ceramic, aluminum, and wood substrates, this growth does not seem to slow down significantly during the time of measurement. A rapid gain in adhesion strength is observed on ceramic and aluminum surfaces, reaching 239.95 kPa and 239.27 kPa within the first 3 h after application underwater, respectively. At such an early stage, the adhesion on glass and polymer substrates is unmeasurable. For these two substrates, 90% of the strength was obtained from 3 h to 12 h.

In Fig. 4a, we summarize the adhesion strength reported by previous literature as a function of the substrate.[8,25,28–34] In general, our nanocomposite adhesives present a universally outstanding underwater bonding ability on diverse substrates. In particular, the hydrogel adhesives outperform every adhesive by fairly large margins when applied to ceramic, glass and wood. The recently developed mussel inspired poly(catechol-styrene) adhesive[8] may be one of the strongest underwater adhesives found to date, which performs comparably well with our nanocomposite adhesives on both aluminum and TPFE substrates, yet our nanocomposite adhesives still exhibit superior adhesion on wood substrates. Detailed values of the adhesion data are listed in Table S2 (ESI†). Two pioneering works of Haraguchi *et al.*[13] and Rose *et al.*[14] also involve the inorganic nanoparticles to strengthen the hydrogel and to glue polymers. The former shows that the nanocomposite type PNIPA hydrogels exhibit extraordinary mechanical properties and the tensile modulus and tensile strength are almost proportional to the clay content, which can be raised up to 305 kPa. The latter shows the adhesion strength to be around 0.22 kPa. Although the performance of the nanocomposite adhesives is marginally better, it is hard to make a rigorous comparison due to the differences in applications of these studies.

In order to have the benchmarks for direct comparison, we evaluated the bonding durability of multiple strongest commercial products with a wide range of compositions, which were particularly designed for wet applications. The same quantity of each adhesive was applied on aluminum substrates underwater and cured in water at 23 °C until measured. Loctite, Aron Alpha and the nanocomposite hydrogel presented similar strong adhesion strengths initially. However, the adhesion strength of the first two products declined significantly over time. After 7 days of curing in water, only about 50% of the strength remained. A similar trend is observed for 3 M Marine and Gorillar Glue but the strength reduction is much less. In contrast, the hydrogel adhesives not only have the highest initial adhesion strength, but also are able to endure long-term immersion under water. Benefitting from the hydration process of ye'elimite which requires the existence of water, one exciting feature of this nanocomposite adhesive is the continuous gain of adhesion strength rather than losing the bonding capacity with time like ordinary glues.

In summary, we demonstrate a hybrid nanocomposite with fast, strong and durable underwater adhesion on diverse surfaces.

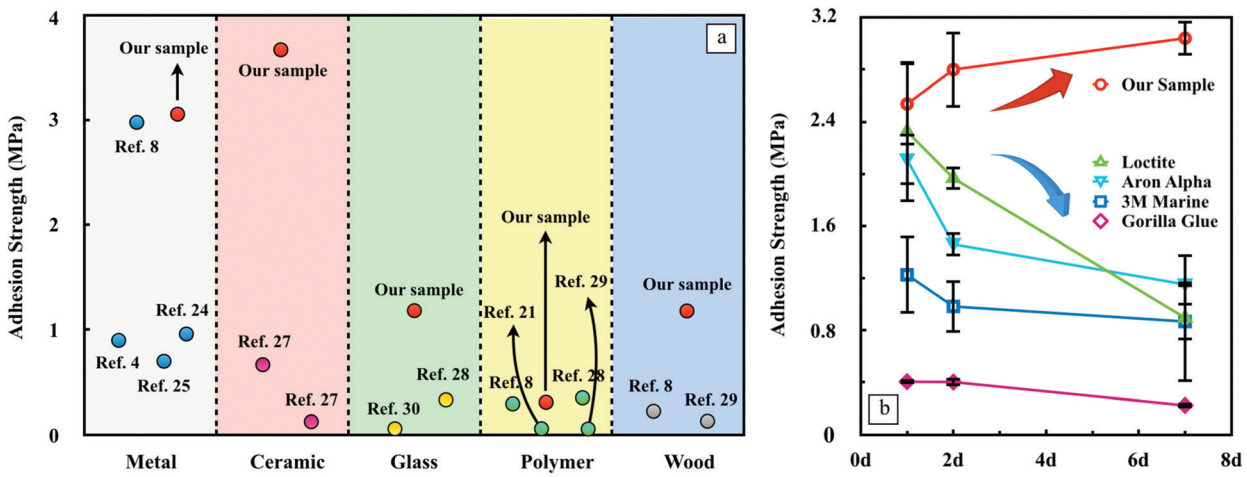

Fig. 4 Benchmarking underwater bonding performance of nanocomposite adhesives. (a) Underwater bonding of nanocomposite adhesives compared to other adhesives reported in the literature. (b) Adhesion strength of nanocomposite adhesives as a function of time used underwater in comparison with the commercial products. Lap shear joints were between aluminum substrates.

The adhesion properties are derived from the characteristics of the two components: hydrogel and ye'elimite. The excellent water absorbing capacity and the highly reversible stretchability of the hydrogel maximize the efficient contact area between adhesives and substrates, and also increase the energy dissipation during debonding. The long-lasting hydration process provides a source of reinforced nanocrystals for the adhesives. Therefore, a durable and sustainable increase in adhesion strength is presented when serving under water, whereas all the commercial products examined in this work exhibit a continuous decline in adhesion performance. The nanocrystals, as a consequence of the ye'elimite hydration process, strengthen the matrix itself and also enhance the physical anchorage at the interface. These merits endow the nanocomposite adhesives with superior underwater bonding properties compared to other commercial products. With this general design strategy which focuses on optimizing the advantages of each component contained, the hydrogel adhesives can be applied directly underwater and present a universal bonding solution to diverse surfaces underwater. This strategy can also be extended to other substrates that are not studied in this work.

Conflicts of interest

There are no conflicts to declare.

Acknowledgements

The authors would like to acknowledge the financial support from the Natural Science Foundation of Jiangsu Province (grant BK20180407), the National Natural Science Foundation of China (No. 51890904, 1706222, 51903047, 51731004 and 51708108), the State Key Laboratory of High Performance Civil Engineering Materials Open Fund (No. 2018CEM001), and the Fundamental Research Funds for the Central Universities.

References

1 R. J. Stewart, T. C. Ransom and V. Hlady, Natural underwater adhesives, *J. Polym. Sci., Part B: Polym. Phys.*, 2011, **49**, 757–771.
2 B. P. Lee, P. B. Messersmith, J. N. Israelachvili and J. H. Waite, Mussel-Inspired Adhesives and Coatings, *Annu. Rev. Mater. Res.*, 2011, **41**, 99–132.
3 H. J. Meredith and J. J. Wilker, The Interplay of Modulus, Strength, and Ductility in Adhesive Design Using Biomimetic Polymer Chemistry, *Adv. Funct. Mater.*, 2015, **25**, 5057–5065.
4 A. H. Hofman, I. A. van Hees, J. Yang and M. Kamperman, Bioinspired Underwater Adhesives by Using the Supramolecular Toolbox, *Adv. Mater.*, 2018, **30**, 1704640.
5 B. P. Lee and S. Konst, Novel hydrogel actuator inspired by reversible mussel adhesive protein chemistry, *Adv. Mater.*, 2014, **26**, 3415–3419.
6 L. Han, *et al.*, Mussel-Inspired Adhesive and Conductive Hydrogel with Long-Lasting Moisture and Extreme Temperature Tolerance, *Adv. Funct. Mater.*, 2018, **28**, 1–12.
7 J. J. Wilker, Biomaterials: Redox and adhesion on the rocks, *Nat. Chem. Biol.*, 2011, **7**, 579–580.
8 M. A. North, C. A. Del Grosso and J. J. Wilker, High Strength Underwater Bonding with Polymer Mimics of Mussel Adhesive Proteins, *ACS Appl. Mater. Interfaces*, 2017, **9**, 7866–7872.
9 R. J. Stewart, C. S. Wang and H. Shao, Complex coacervates as a foundation for synthetic underwater adhesives, *Adv. Colloid Interface Sci.*, 2011, **167**, 85–93.
10 G. P. Maier, M. V. Rapp, J. H. Waite, J. N. Israelachvili and A. Butler, Adaptive synergy between catechol and lysine promotes wet adhesion by surface salt displacement, *Science*, 2015, **349**, 628–632.
11 J. Wang, C. Liu, X. Lu and M. Yin, Co-polypeptides of 3,4-dihydroxyphenylalanine and l-lysine to mimic marine adhesive protein, *Biomaterials*, 2007, **28**, 3456–3468.
12 B. J. Kim, *et al.*, Mussel-mimetic protein-based adhesive hydrogel, *Biomacromolecules*, 2014, **15**, 1579–1585.
13 K. Haraguchi, T. Takehisa and S. Fan, Effects of clay content on the properties of nanocomposite hydrogels composed of poly(N-isopropylacrylamide) and clay, *Macromolecules*, 2002, **35**, 10162–10171.
14 S. Rose, *et al.*, Nanoparticle solutions as adhesives for gels and biological tissues, *Nature*, 2014, **505**, 382–385.
15 X. Tong, L. Du and Q. Xu, Tough, adhesive and self-healing conductive 3D network hydrogel of physically linked functionalized-boron nitride/clay/poly(N-isopropylacrylamide), *J. Mater. Chem. A*, 2018, **6**, 3091–3099.
16 A. Cholewinski, F. Yang and B. Zhao, Algae-mussel-inspired hydrogel composite glue for underwater bonding, *Mater. Horiz.*, 2019, **6**, 285–293.
17 N. Manuja, R. Nagpal and I. K. Pandit, Dental adhesion: Mechanism, Techniques and Durability, *J. Clin. Pediatr. Dent*, 2012, **36**, 223–234.
18 K. S. Sivudu and K. Y. Rhee, Preparation and characterization of pH-responsive hydrogel magnetite nanocomposite, *Colloids Surf., A*, 2009, **349**, 29–34.
19 K.-F. Arndt, A. Richter, S. Ludwig, J. Zimmermann, J. Kressler and D. Kuckling, Poly(vinyl alcohol)/poly(acrylic acid) hydrogels: FT-IR spectroscopic characterization of crosslinking reaction and work at transition point, *Acta Polym.*, 1999, **50**, 383–390.
20 Q. Tang, J. Wu, H. Sun, J. Lin, S. Fan and D. Hu, Polyaniline/polyacrylamide conducting composite hydrogel with a porous structure, *Carbohydr. Polym.*, 2008, **74**, 215–219.
21 J. Chang, J. Li, J. Han and T. Zhang, Traces of CH in a C4A3$$-C2S hydration system, *Constr. Build. Mater*, 2019, **197**, 641–651.
22 P. W. Shum, Z. F. Zhou, K. Y. Li and Y. G. Shen, XPS, AFM and nanoindentation studies of Ti1-xAlxN films synthesized by reactive unbalanced magnetron sputtering, *Mater. Sci. Eng., B*, 2003, **100**, 204–213.
23 C. W. Jennings, Surface roughness and bond strength of adhesives1, *J. Adhes.*, 1972, **4**, 25–38.
24 W. Song, A. Gu, G. Liang and L. Yuan, Effect of the surface roughness on interfacial properties of carbon fibers reinforced epoxy resin composites, *Appl. Surf. Sci.*, 2011, **257**, 4069–4074.
25 Y. Ma, *et al.*, Remote Control over Underwater Dynamic Attachment/Detachment and Locomotion, *Adv. Mater.*, 2018, **30**, 1–8.

26 K. L. Mittal, *Progress in Adhesion and Adhesives*, 2015, DOI: 10.1002/9781119162346.
27 A. Pizzi, Recent developments in eco-efficient bio-based adhesives for wood bonding: Opportunities and issues, *J. Adhes. Sci. Technol.*, 2006, **20**, 829–846.
28 C. L. Jenkins, H. M. Siebert and J. J. Wilker, Integrating Mussel Chemistry into a Bio-Based Polymer to Create Degradable Adhesives, *Macromolecules*, 2017, **50**, 561–568.
29 H. Shao and R. J. Stewart, Biomimetic underwater adhesives with environmentally triggered setting mechanisms, *Adv. Mater.*, 2010, **22**, 729–733.
30 S. Kaur, G. M. Weerasekare and R. J. Stewart, Multiphase adhesive coacervates inspired by the sandcastle worm, *ACS Appl. Mater. Interfaces*, 2011, **3**, 941–944.
31 H. J. Kim, B. H. Hwang, S. Lim, B. H. Choi, S. H. Kang and H. J. Cha, Mussel adhesion-employed water-immiscible fluid bioadhesive for urinary fistula sealing, *Biomaterials*, 2015, **72**, 104–111.
32 P. G. Lawrence and Y. Lapitsky, Ionically cross-linked poly(allylamine) as a stimulus-responsive underwater adhesive: Ionic strength and pH effects, *Langmuir*, 2015, **31**, 1564–1574.
33 A. Li, *et al.*, Mineral-Enhanced Polyacrylic Acid Hydrogel as an Oyster-Inspired Organic-Inorganic Hybrid Adhesive, *ACS Appl. Mater. Interfaces*, 2018, **10**, 10471–10479.
34 P. Rao, *et al.*, Tough Hydrogels with Fast, Strong, and Reversible Underwater Adhesion Based on a Multiscale Design, *Adv. Mater.*, 2018, **30**, 1–8.

